CCFE
CULHAM CENTRE FOR FUSION ENERGY

UK Atomic Energy Authority

UKAEA-CCFE-PR(22)31

HJ. Sun, SA. Silburn, IS. Carvalho, C Giroud, G Fishpool, GF. Matthews, DB. King, RB. Henriques, DL. Keeling, FG. Rimini, L. Garzotti, D. Frigione, D. Van Eester, D Kos, M-L. Mayoral, J. Mailloux, C. Maggi, A. Huber, D. Douai, PJ. Lomas, L Morten, M. Maslov, K. Kirov, P. Jacquet, CG. Lowry, M. Baruzzo, C. Stuart, J. Mitchell, L. Horvath, DC. McDonald, JET Contributors

The broadening of SOL profiles in JET tritium plasma and its impact on machine operation

The broadening of SOL profiles in JET tritium plasma and its impact on machine operation

HJ. Sun, SA. Silburn, IS. Carvalho, C Giroud, G Fishpool, GF. Matthews, DB. King, RB. Henriques, DL. Keeling, FG. Rimini, L. Garzotti, D. Frigione, D. Van Eester, D Kos, M-L. Mayoral, J. Mailloux, C. Maggi, A. Huber, D. Douai, PJ. Lomas, L Morten, M. Maslov, K. Kirov, P. Jacquet, CG. Lowry, M. Baruzzo, C. Stuart, J. Mitchell, L. Horvath, DC. McDonald, JET Contributors

This is a preprint of a paper submitted for publication in Nuclear Fusion

The broadening of SOL profiles in JET tritium plasma and its impact on machine operation

HJ. Sun[1], SA. Silburn[1], IS. Carvalho[2], C Giroud[1], G Fishpool[1], GF. Matthews[1], DB. King[1], RB. Henriques[1], DL. Keeling[1], FG. Rimini[1], L. Garzotti[1], D. Frigione[3], D. Van Eester[4], M. Groth[5], J. Flanagan[1], D Kos[1], A. Boboc[1], P. Shi[1], M-L. Mayoral[1], J. Mailloux[1], C. Maggi[1], A. Huber[6], D. Douai[7], N. Vianello[8], PJ. Lomas[1], L Morten[1], M. Maslov[1], K. Kirov[1], P. Jacquet[1], CG. Lowry[1], M. Baruzzo[9], C. Stuart[1], J. Mitchell[1], L. Horvath[1], DC. McDonald[1], and JET Contributors[10]

[1]UKAEA/CCFE, Culham Science Centre, Abingdon, Oxon, OX14 3DB, UK
[2]General Atomics, PO Box 85608, San Diego, CA 92186-5608, United States of America
[3]Universit`a di Roma Tor Vergata, Via del Politecnico 1, Roma, Italy
[4]Laboratory for Plasma Physics LPP-ERM/KMS, B-1000 Brussels, Belgium
[5]Aalto University, PO Box 14100, FIN-00076 Aalto, Finland
[6]Forschungszentrum Jülich GmbH, Institut für Energie- und Klimaforschung, Plasmaphysik, 52425 Jülich, Germany
[7]CEA, IRFM, F-13108 Saint Paul Lez Durance, France
[8]Consorzio RFX, Corso Stati Uniti 4, 35127 Padova, Italy
[9]Dip.to Fusione e Tecnologie per la Sicurezza Nucleare, ENEA C. R. Frascati, via E. Fermi 45, 00044 Frascati (Roma), Italy
*[10]See the author list of J. Mailloux et al 2022 Nucl. Fusion **62** 042026*

e-mail contact of the main author: HongJuan.SUN@UKAEA.UK

Abstract.

Unusually high power loads on the Beryllium limiter caused by Neutral Beam re-ionisation, and much cooler divertor target surfaces were observed during the recent JET tritium campaign. As both phenomena are driven by scrape-off layer (SOL) physics, the SOL features of 72 tritium H-mode discharges and their deuterium references have been studied.

The majority (70) of tritium H-mode discharges had usual exponentially decaying SOL profiles. The tritium plasmas are observed to have increased separatrix density and collisionality than their deuterium references. This is associated with $\approx 2-3$ times broader SOL width for both density and temperature profiles. This is consistent with previous observation in highly collisional deuterium H-mode plasma on AUG [Sun, PPCF, 2015] and interpreted as high collisionality enhancing cross-field transport across the separatrix and resulting in broadening of near SOL above a critical value. The other two tritium H-mode discharges had near flat SOL density profiles, similar to the so-called '*density shoulder formation*' observed in L-mode plasma. The SOL collisionality of these two pulses lies within the range of T pulses without density shoulder formation. This supports the conclusion of previous studies [Vianello, NF, 2017; Wynn, NF, 2018] that increased collisionality is not sufficient for the formation of a

'*density shoulder*' and additional factors, likely divertor condition or interaction with neutrals, are required.

JET tritium plasma provides evidence of favourable and unfavourable effects of enhanced cross-field SOL transport on machine operation. The larger limiter power loads due to re-ionisation of Neutral Beam Injection observed in the T pulses relative to their D references has been shown to be consistent with the combined effects of the broadening of the SOL profile and larger beam ion Larmor radius. The enhanced cross-field particle transport and the resulting broader SOL width provides more particles to ionize the fast Beam neutrals, causing the unfavourable power load issue on the Beryllium limiter. The broader near SOL profiles of the T plasma spreads the heat load over a larger area and, together with the increased separatrix density, results in a favourably cooler divertor target.

PACS numbers: 52.25.Fi, 52.50.Gj

1 Introduction

The properties of the scrape-off layer (SOL) play a crucial role on some of the most important operational aspects of present-day tokamak and on the design of fusion power plants. It is widely observed that the SOL profiles normally exhibit a two-zone structure: a steep gradient region in density and temperature near the separatrix (near SOL) and a flatter profile region (far SOL) further towards the first wall. The energy transport is generally dominated by parallel conduction in the near SOL region, where most of the power and particles flows and exhausts to the divertor surface. Thus, the amount of divertor target surface involved in plasma power and particle exhaust is largely determined by the width of the near SOL profile. In the far SOL the cross-field transport is large and convective, resulting in much broader profiles in this region. The far SOL region can be important for directly affecting the plasma-wall interaction in the main chamber if the plasma is sufficiently hot and dense enough.

The SOL heat flux width determines the region of the divertor target over which the power exhaust is spread and so is a critical parameter for determining whether the power exhaust is compatible with acceptable wall loads. Multi-machine studies show that the most important scaling parameter for SOL heat flux width, λ_q, is the poloidal magnetic field, B_{pol}, (or equivalently the plasma current, I_p), with λ_q decreasing linearly with increasing B_{pol} [1]. This causes a significant concern for ITER operation, as a heat flux width of $\sim 1\ mm$ is predicted for ITER at $I_p = 15\ MA$, which may induce unbearable heat flux to the target surface. Later

experimental observation on AUG shows that a simultaneous broadening of upstream temperature and density SOL profiles for H-mode plasma appears at high separatrix density or collisionality [2]. The region of power exhaust starts from separatrix and lies mainly in the near SOL, while the two-zone SOL structure is maintained. Because of the importance of power exhaust, the near SOL region and its width have been extensively studied experimentally, theoretically, and through simulation to seek scenarios beneficial for both power exhaust and good confinement [3] [4] [5] [6] [7] [8]. Simulations by the XGC1 code predict a significant broadening of the SOL power width for ITER due to it entering a regime of enhanced cross-field transport [9]. Broadly, two classes of mechanism are seen to lead to enhanced transport across the separatrix at higher collisionality. The first results from increased collisional damping of zonal flows due to the increasing of plasma density, thus inhibiting the self-regulation of turbulence and transport of particles [10] [11] [12] [13]. The second results from the development of additional instabilities, such as resistive MHD modes [14] [15] [10] [6] [16]. As collisionality increases, the plasma enters the resistive regime, the perpendicular transport is enhanced by resistive modes.

It has been observed in L-mode plasma that, when the Greenwald density fraction, f_{GW}, is larger than a certain value, the flat region in density profile extends gradually from far SOL to the near SOL region, eventually reaching the separatrix. The phenomenon has been called the L-mode high density transition (HDT) or '*density shoulder formation*'. This feature of SOL profile flattening was first observed in AUG [17] and first related to enhanced perpendicular convective particle transport in studies from C-mod [18]. The enhanced cross-field particle transport has important implication regarding sputtering of first-wall material and recycling fuelling for future devices. It has since been widely observed and studied on many fusion devices [19] [20] [21] [22] [23] [24]. The onset of the extension of the flat region is generally accepted to be caused when, at sufficiently high collisionality, cross-field particle transport becomes dominated by elongated convective cells, known as filaments or blobs, which increase diffusivity. Later studies [25] [26] suggest that increased collisionality is not sufficient condition for establishment of shoulder formation and other factors, like neutrals or divertor recycling, may play a role in it. Although the density profile broadens significantly after density shoulder formation, the temperature profile in the near SOL region is generally observed to remain unchanged [27]. However, a study on AUG [28] did find an increase of heat transport in the far SOL which was associated with filamentary activity after the shoulder formation. More recently, it is observed that the increased filamentary activity may contribute to the

broadening of the power decay length in strongly shaped H-mode plasma regime, known as quasi continuous exhaust regime [4] [29] [30].

This paper reports the observation of SOL broadening in plasmas from the JET T campaign and provides the experimental evidence of detrimental and beneficial effect on machine operation by enhanced cross field transport. The rest of this paper is organized as follows: the experimental setup and plasma wall protection system are introduced in section 2. In section 3, by comparing JET T plasma with their D references, the observations of unusual high re-ionisation rate, cooler divertor target, and underlying SOL properties are reported and their interplay discussed. In Section 4, the results are summarised and implications discussed.

2 NBI re-ionization issue and real-time protection system of JET ILW

Neutral Beam Injection (NBI) is one of the major external heating methods used on JET. Injected energetic neutral particles are ionized in the target plasma by atomic physics processes. The resulting energetic ions are confined in the tokamak's magnetic field and subsequently transfers the energy to the bulk target plasma through Coulomb collisions. However, before the energetic neutral particles reach the target plasma, a fraction of them are ionised through interactions with the background gas in the beam duct and the neutrals and plasma in the SOL region. As the fast neutral particles started life as ions before they were neutralised in the gas neutraliser, this process is referred to as re-ionization. Re-ionization in the duct, near the wall and in the SOL region results in power load to in-vessel components which will result in damage if it becomes excessive. The re-ionization rate in the NBI duct is proportional to the gas density. The ionized energic particles will be deflected by magnetic field and cause excessive power load inside duct at a certain density or pressure. To protect against this, the gas pressure in the JET NBI ducts is monitored by a Penning gauge and NBI will be stopped if the pressure is higher than a trip level (1.2×10^{-5} mbar).

Re-ionisation can also occur in the main chamber and SOL region just outside the NBI duct, with the potential to damage the beryllium limiter. To avoid damage of the beryllium limiter by events such as re-ionisation, real-time protection of the ITER-like wall based on near infrared imaging diagnostic systems has been implemented on JET since 2011 [31] [32]. Analog CCD cameras with near infrared wavelength are used to measure surface temperature of the plasma facing components. The maximum temperature measured in each region of interest (ROI) is sent to the vessel thermal map (VTM). If the temperature reaches the alarm threshold (trip

level), the VTM requests an appropriate response from the plasma control system by sending an alarm to the real time protection sequencer (RTPS). This controls the actuators and then safely terminates the plasma, thereby reducing the risk of beryllium melting or tungsten cracking. In later DT campaign, switching off certain PINIs has been implemented as an alternative protection scheme to minimize the loss of scientific output. Figure 1 shows the region of interest (ROI) chosen to protect against re-ionisation for the JET-ILW. Here, different colours represent the different materials of the first wall: green for beryllium and orange for W-coated CFC. The ROI denoted BEION4 represents the Beryllium limiter in octant 4 which is protected against re-ionization events. The ROI denoted REION4 represents the Tungsten coated CFC in octant 4 which is similarly protected against re-ionization events. Although, the typical alarm temperature threshold for Beryllium is 925 ℃ , the alarm threshold for BEION4 is cautiously set as 850 ℃ as the limiter wall temperature can increase very quickly when re-ionisation occurs. Figure 2 shows the ROI chosen to protect the divertor target surface. Here, DVWC stands for divertor W coated tiles and DVWB for divertor bulk tungsten tile, which is used to study the divertor surface temperature increase in this paper.

The general characteristics and machine conditions for the JET T campaign can be found in Ref [33] [34]. The high-resolution Thomson scattering (HRTS) diagnostic [35] [36] provides the main measurement for analysis of electron density (n_e) and electron temperature (T_e) profiles as in Ref [37].

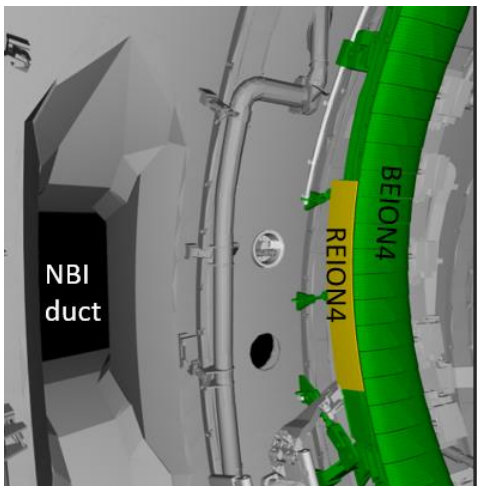

Figure 1. Wall segments protected against re-ionisation. BEION 4: beryllium limiter in Octant 4. REION4: tungsten coated CFC.

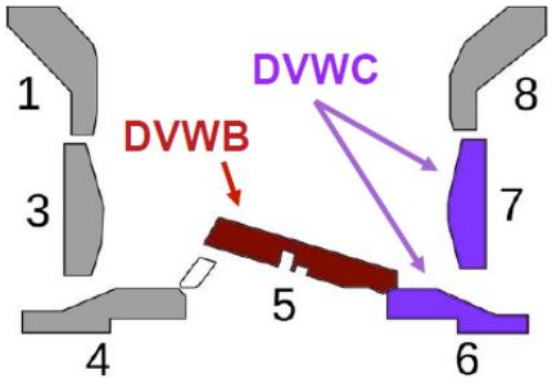

Figure 2. Segments protected against melting of divertor target surface. DVWC, Divertor tungsten coated tiles, DVWB: Divertor bulk tungsten tiles

3 Experimental observations

3.1 Higher re-ionisation rate and cooler divertor target during JET tritium campaign

The JET pure T campaign started at the beginning of 2021 and ended in March, 2022. It was divided into two parts: before and after the DT campaign (Aug to Dec, 2021). To maximize the experimental output, all the T pulses are based on good performance deuterium (D) reference pulses, such that the plasma configuration, heating scheme, global parameters, and gas injection locations match those of the D reference pulse. Although all the D reference pulses have good performance, the T campaign had an unusually high number of discharges where the limiter temperature caused by beam re-ionisation issue reached the alarm threshold and the plasma was terminated earlier than expected. This affected the general scientific output of T campaign. The study in this paper is motivated by the unusual high re-ionisation rate. A database of 72 discharges with relatively good NBI performance are selected from the first part of the JET T campaign. The protection camera used to monitor re-ionisation in Octant 8 for the protection system was removed prior to the DT campaign as it is not DT compatible. It was only reinstalled towards the end of the second part of the T campaign. In addition, NBI PINIs in octant 4 were not used due to technical issues during the second part of the T campaign. To ensure consistency of diagnostics and heating location, pulses from the second part of the T campaign are not included in the database here. Among the selected 72 pulses, 18 pulses terminated due to excessive re-ionisation.

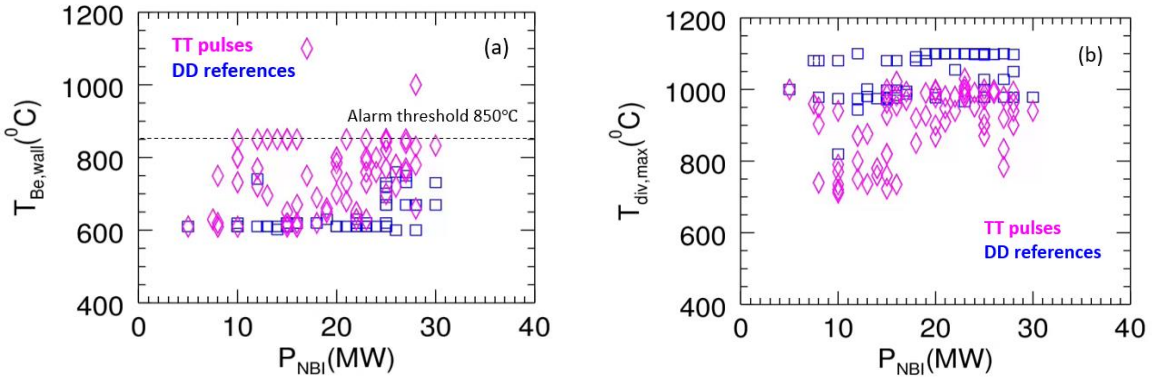

Figure 3. (a)Wall surface temperature $T_{Be,wall}$ (ROI: BEION4) caused by re-ionisation issue against total NBI heating power. (b) divertor target surface temperature $T_{div,max}$ (ROI: DVWC or DVWB) against total NBI heating power. Blue squares are DD reference pulses and magenta diamonds are TT pulses.

In figure 3(a), blue squares are DD reference pulses and magenta diamonds are TT pulses. The wall temperature is taken from BEION4 (figure 1), as it has the best sensitivity and highest accuracy. The pulses with $T_{Be,wall} \geq 850℃$ were terminated prematurely to avoid melting the Beryllium wall. Although many of the T plasma in the dataset didn't reach the alarm threshold, the wall surface temperature is generally much higher for T pulses compared with their D references, with no strong correlation with NBI power. Although the power load caused by beam re-ionisation is much worse, the divertor target surface temperature is much cooler in T plasma, as shown in figure 3(b). In figure 3(b), the target surface temperature is the maximum value in the pulse taken from DVWC and DVWB (figure 2). For a given NBI heating power, the divertor target is cooler for the T plasma indicating that the plasma SOL characteristics are different. This suggests that the main reason for higher re-ionisation in the T plasma may be the change of SOL condition, instead of T energetic neutral beam itself.

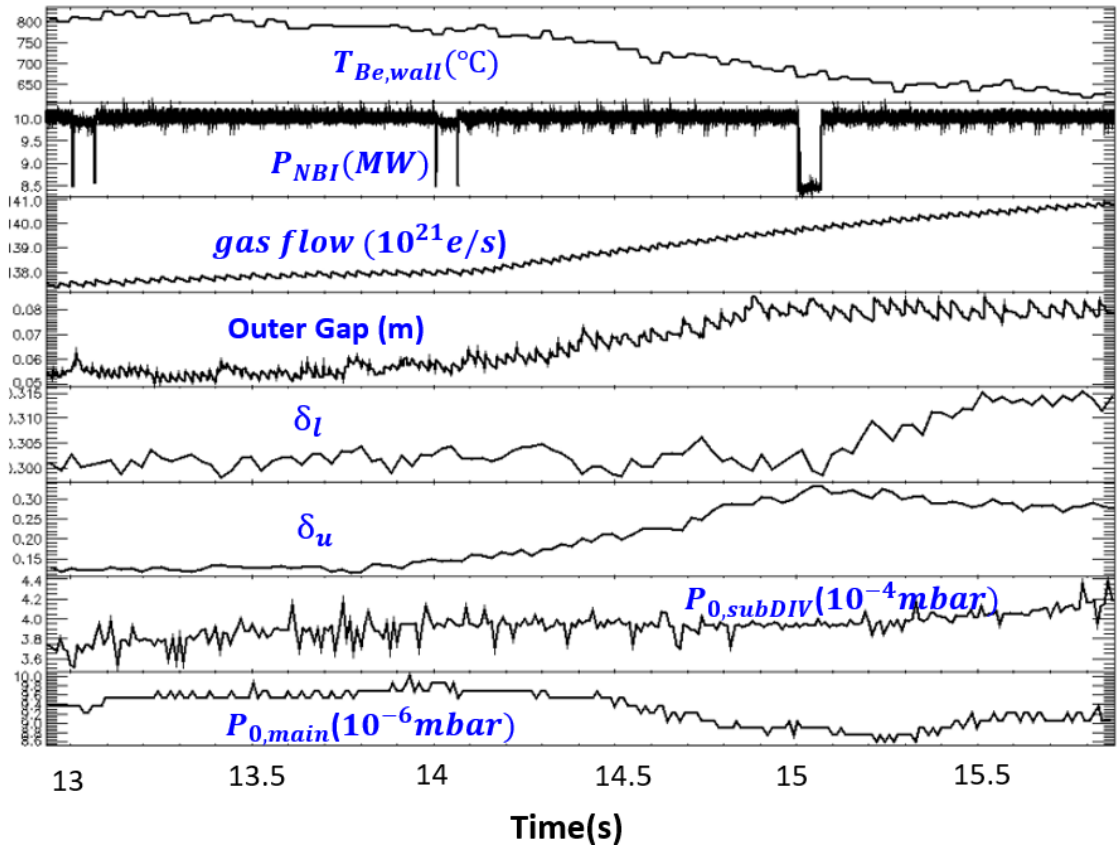

Figure 4. Time traces of JET T pulse #98794: Beryllium wall surface temperature ($T_{Be,wall}$) next to NBI duct, NBI total heating power (P_{NBI}), injecting gas flow and radial outer gap, low and upper triangularity (δ_l and $\bar{\delta}_u$), neutral pressure in sub-divertor ($P_{0,subDIV}$) and neutral pressure in the main chamber ($P_{0,main}$).

The often-used method to mitigate the re-ionisation issue is moving plasma away from the wall by increasing the radial outer gap (ROG). An example of such as pulse, #98794, is given in figure 4. In the discharge, the Be wall temperature has risen to ≈ 800 ℃ at 10 s. The outer gap is increased from 5 cm to 8 cm by 11 s and the Be wall temperature decreases despite the total heating power remaining almost unchanged. However, increasing the outer gap is not always so effective. In figure 4, the upper triangularity increases at the same time as the outer gap increases, so the whole plasma moves away from outer wall. During this time, the neutral pressure in the main chamber decreases while the total gas flow slightly increases. The observation that increasing the clearance between plasma and first wall mitigates the re-ionisation issue further supports the idea that the phenomena is not caused by the characteristics of tritium beam itself. During the JET T campaign, the gas flow was often increased during H-mode to raise the ELM frequency to flush impurities. This was because pellet pacing, the standard technique for ELM control in D plasma, could not be used as the pellet launcher is not compatible with T operation.

It might be expected that higher gas flow in T plasma could account for the higher re-ionisation levels. However, as can been seen in figure 5, there are pulses with very high line integrated density (i.e., high gas level) with no re-ionisation issue, while some of pulses terminated due to re-ionisation have relatively low density. The re-ionisation issue is not purely determined by gas injection level.

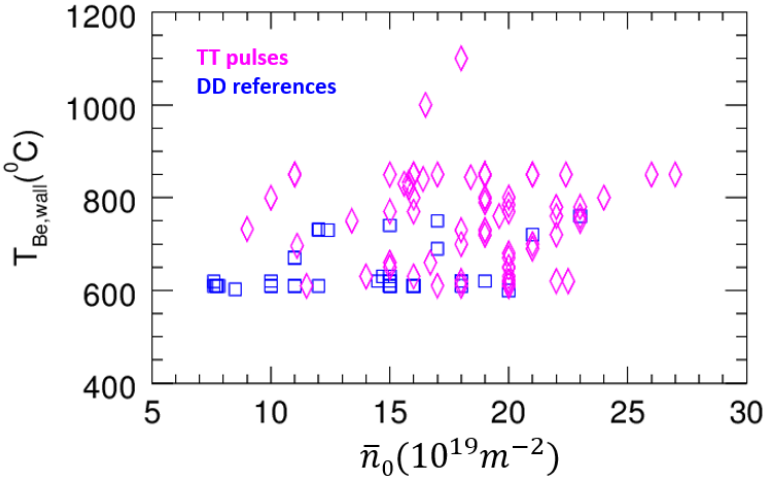

Figure 5. Maximum wall surface temperature for the octant 4 Be limiter (BEION4), driven by re-ionisation, against line integrated density. Blue squares are DD reference pulses and magenta diamonds are TT pulses.

The divertor target temperature and the observed power load caused by beam re-ionisation issue on the main chamber, both key parameters for plasma operation, clearly depend on the SOL properties. This motivates the study of the differences in SOL properties between the JET T discharges and their D references.

3.2 Observed broadening of SOL profiles in JET tritium plasma

For the worst re-ionisation pulses in the JET T plasma, the types of SOL broadening were observed: one without density shoulder and one with density shoulder. Their behaviour is outlined and discussed in the following sections.

3.2.1 The feature of SOL broading without density shoulder formation

The majority of T plasma in the dataset (70 from 72), and all the D references, exhibited SOL profiles with exponentially decaying SOL density and temperature profiles, similar to previous observations on AUG [2]. Figure 6 shows time traces of such a T pulse (#98901, red), which was terminated due to excessive power load by re-ionisation issue, and its D reference (#97886, blue). The gas flow is almost identical for the two discharges, except that the gas is injected $300\ ms$ earlier in the T pulse than in the reference. It is empirically found the T gas injection modules are generally $300\ ms$ slower than the D gas injection modules. To account for this, gas injection is timed to start $300\ ms$ earlier in the T pulses than their D references. Although both timing and heating power of NBI, and radial outer gap remain the same for the two pulses, the wall temperature increases soon after the injection of NBI for the T pulse and the pulse is terminated at about 9.7s. Figure 7 shows the profiles of the T plasma just before the pulse is terminated and the profiles of its D reference at the same time. The profiles have been shifted $\approx 1\ cm$ to match the separatrix position ($T_e \approx 100eV$). Even with same gas flow, the density at the edge (inside and outside the separatrix) is higher and the density decay length is broader for the T plasma. The absence of electron temperature measurements for the D reference for $R > 3.81\ m$ is because the electron temperature is below the measurable value (≈20 eV). This implies that the SOL temperature profile decay length is much longer for the T plasma than its D reference.

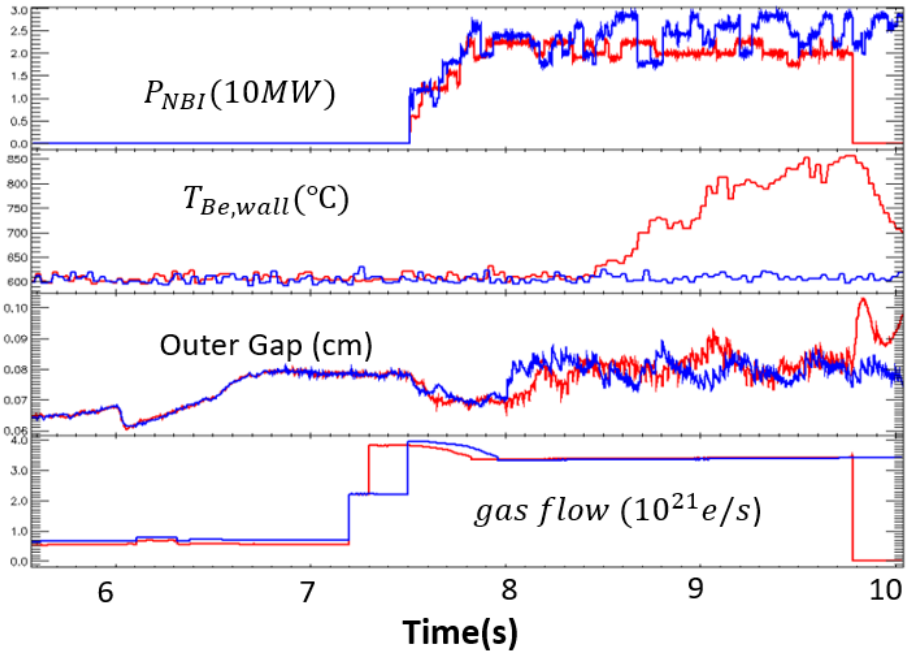

Figure 6. Time traces of JET T pulse #98901 (red) and its D reference #97886(blue): Beryllium wall surface temperature ($T_{Be,wall}$) next to NBI duct, NBI total heating power (P_{NBI}), injecting gas flow and radial outer gap.

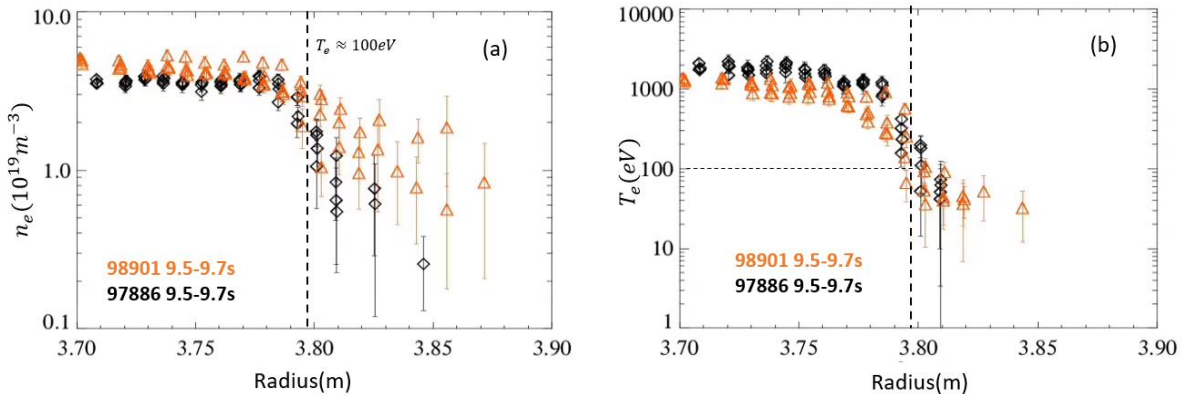

Figure 7. Log-linear plots of the electron temperature and density profiles, for the same JET pulses as in figure 6. (a) edge n_e profile at midplane; (b) edge T_e profile at the midplane. JET T pulse #98901 (in orange) and D pulse #97886 (in black).

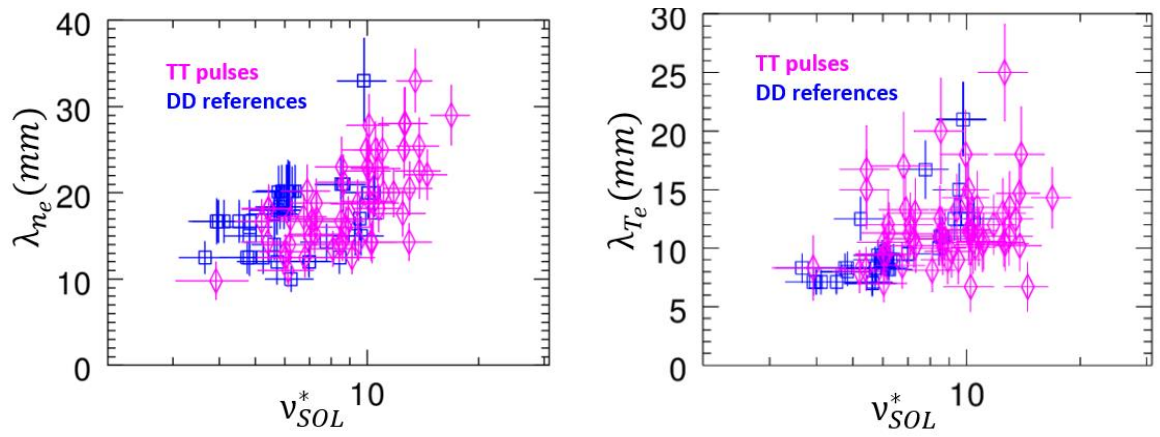

Figure 8. the near SOL density decay length $\lambda_{n_{e,u}}$ (a) and temperature decay length $\lambda_{T_{e,u}}$ (b) for JET T and D plasma against effective SOL collisonality ν^*_{SOL}. Blue squares are DD reference pulses and magenta diamonds are TT pulses.

Across the dataset of the selected JET T pulses without SOL density shoulder formation and their D references, the density decay length in the near SOL region is found to increase with the SOL collisionality, $\upsilon^*_{SOL,e} \approx 10^{-16} n_{e,u} L/T^2_{e,u}$, figure 8(a), with the increase being modest for low SOL collisionality, where it lies in the range $\lambda_{n_e} = 10 - 20$, and becoming stronger above a critical value, $\upsilon^*_{SOL,e} \approx 8$, where λ_{n_e} increases to $2 - 3$ times comparing with low collisionality values. This is in agreement with previous observations on AUG [2] [6]. Across the dataset, a temperature of 100eV is used to determine the separatrix position and $n_{e,u}$ is taken from HRTS measurement at the position. λ_{n_e} for both Deuterium and Tritium plasma has similar trend with SOL collisionality, although tritium plasma has generally higher collisionality. The temperature decay length, figure 8(b), follows a similar general trend, with the SOL broadening as collisionality increases. However, the data look more scattered for the temperature decay length. The greater spread could be an artefact of diagnosis - high density is beneficial for density measurement of HRTS, but the temperature tends to drop below the measurable values in the near SOL region. Thus, the measured SOL temperature decay length is likely less accurate than the SOL density decay length.

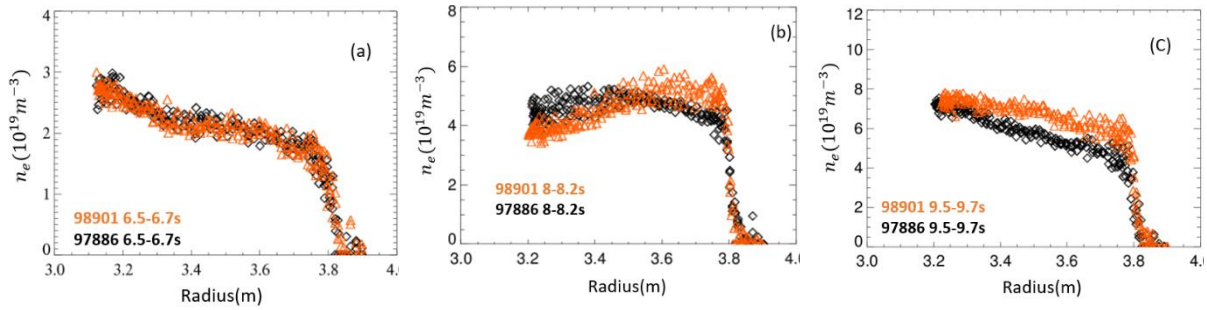

Figure 9. Electron density n_e profile at the various phases for JET T pulse, #98901 (orange), and its D reference pulse, #97886 (black). (a) Ohmic phase before NBI; (b) H-mode phase just after NBI switched on; (c) H-mode phase during re-ionisation, same time as in figure 6.

Figure 9 shows the evolution of the density profiles in the confined region of the two discharges as in figure 6 and figure 7. Before applying any NBI, figure 9(a), the T and D plasma have almost identical profiles across the confined region for the same gas flow. Figure 9(b) shows the density profiles just after L-H transition, $200\ ms$ after applying full NBI power. For the T pulse, the pedestal density is higher and the core density lower than the D reference. The T pulse exhibits a hollow density profile shape. Although a peaked density profile is recovered later in the T pulse, figure 9(c), it is less peaked in the core than its D reference pulse. The separatrix density for the T pulse is higher and SOL profile broader at this time, figure 7. Thus, in the H-mode phase, the density profile of the T plasma is observed to have a greater opacity at the edge than its D reference.

3.2.2 **SOL broadening with density shoulder formation**

Among the 18 pulses terminated by the re-ionisation issue, two of the JET T plasma in the dataset were observed to have SOL density shoulders. Both exhibited large heat loads on the Be limiter due to reionisation leading to rapid termination of the pulse. Figure 10 shows the characteristic time traces for one of these JET T pulses together with its D reference which had no significant reionisation issues. This is an example of a T pulse where, in contrast to its D reference, increased gas flow has been used to modify ELM frequency for impurity control. Although the total NBI power for the T pulse (red) is slightly less than its D reference (blue), the wall temperature increases rapidly from ≈10.8 s until it reaches the alarm threshold, 850 ℃, and the plasma is terminated by the JET protection system at ≈11.2 s. The time taken for reionisation to raise the limiter temperature by 200 ℃ is ≈ $400\ ms$ which is significantly faster than for the plasma with exponentially decaying SOL profiles, such as #98901 which takes ≈ $2\ s$, figure 6.

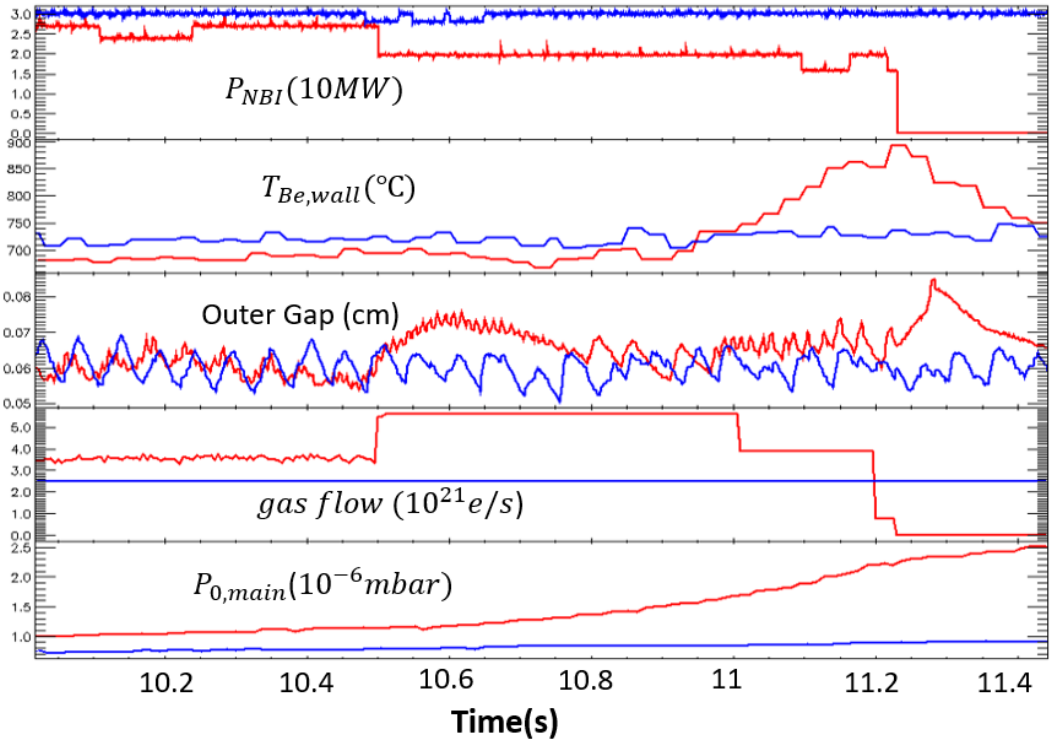

Figure 10. Time traces of JET T pulse #99170 (red) and its D reference #97845(blue): Beryllium wall surface temperature ($T_{Be,wall}$) next to NBI duct, NBI total heating power (P_{NBI}), injecting gas flow and radial outer gap, low and upper triangularity (δ_l and $\bar{\delta}_u$), neutral pressure in sub-divertor ($P_{0,subDIV}$) and neutral pressure in the main chamber ($P_{0,main}$).

Figure 11 shows the edge electron density and temperature profiles in the SOL region before (a and b) and during the period of excessive re-ionisation power load (c and d). The profiles of the D pulse, #97845, have been shifted so that the position of their separatrices, the location where $T_e \approx 100\ eV$ [37], coincide. Prior to the re-ionisation issue, $t = 10.2\ s$, the density profile shape and length scale across the separatrix look similar for the T and D pulses. The average separatrix density for the T pulse is $\approx 2.2 \times 10^{19}\ m^{-3}$ and is higher than its D reference #97845, $\approx 1.6 \times 10^{19}\ m^{-3}$. During the re-ionization issue, the profiles change significantly in the SOL region. The SOL density profile for the T pulse looks almost completely flat, as for those reported in L-mode plasma in HDT regime [17] [18] [20]. However, unlike the L-mode plasma observed in the HDT regime, the temperature decay length for the T plasma is significantly broadened as well. The absence of temperature measurements for the D reference for $R > 3.81\ m$ is because the electron temperature is below the measurable value (≈20 eV). This implies that the SOL temperature profile decay length is much longer for the T plasma than its D reference. The flat density profile for the T plasma suggests that the cross-field transport in the SOL region is dramatically enhanced and many more particles are brought close or even straight to the wall. This is consistent with, this the significant increase of neutral

pressure in the main chamber seen in figure 10. Consequently, much more energetic neutrals from NBI are re-ionized before they reach the target plasma and cause the power load issue near the NBI duct.

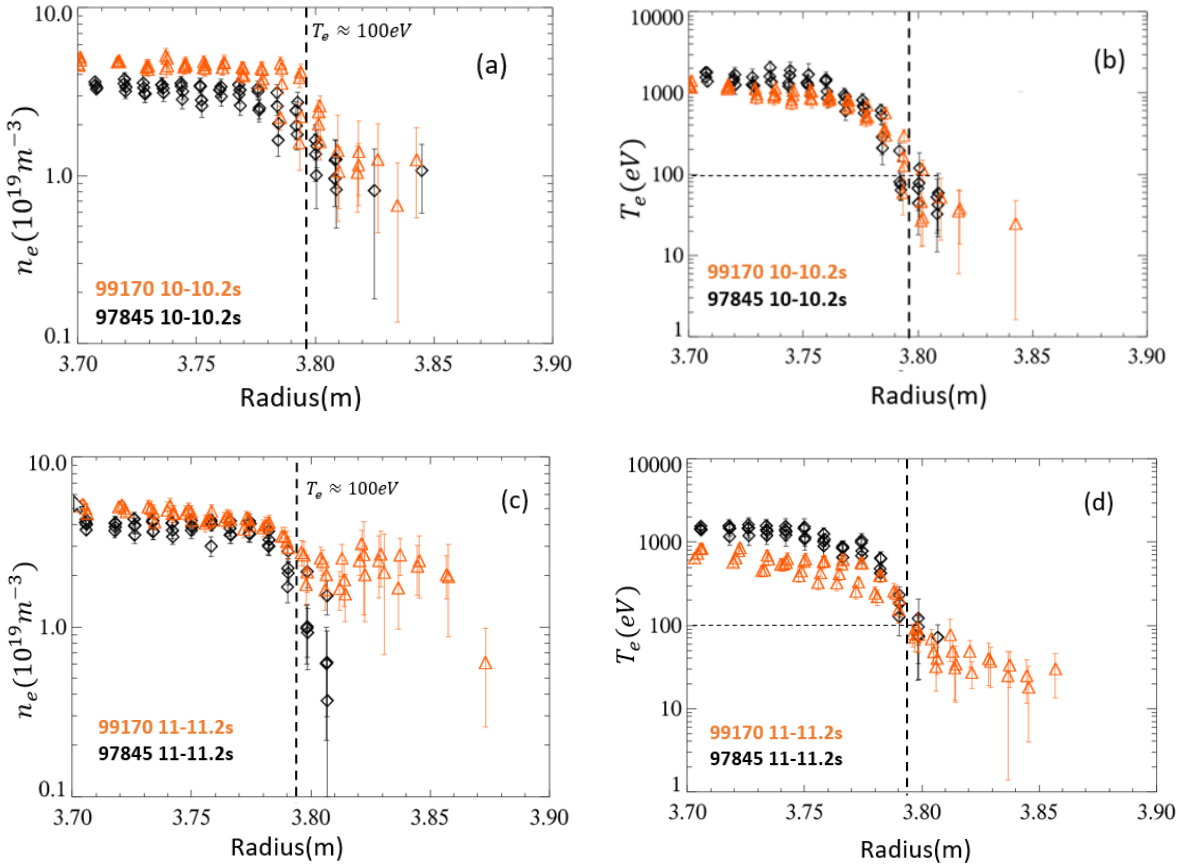

Figure 11. Electron temperature and density profiles for the same JET pulses as in figure 10: (a) edge n_e at the midplane before re-ionisation issue; (b) edge T_e profile at the midplane before re-ionisation issue; (c) edge n_e profile at midplane during re-ionisation issue; (d) edge T_e profile at the midplane before re-ionisation issue. JET T pulse #99170 (in orange) and D pulse #97845 (in black).

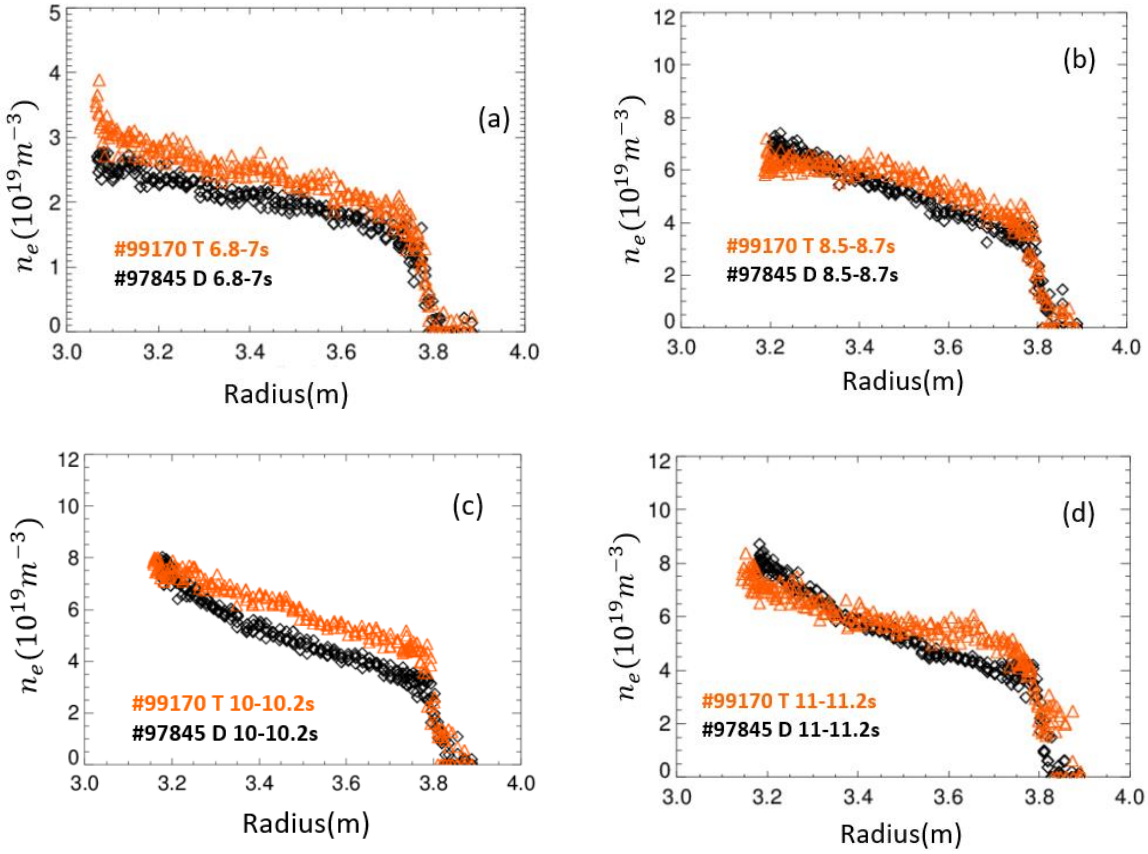

Figure 12. n_e profile at various phases of the JET pulses introduced in figure 10: (a) Ohmic phase before NBI; (b) H-mode phase when NBI just switched on; (c) H-mode phase 1.5s after NBI switched on, same time as figure 11(a) and (b); (d) H-mode phase during re-ionisation issue, same time as in figure 11(c) and 11(d). JET T pulse #99170 (in orange) and D pulse #97845 (in black).

Turning to the evolution of the core and edge density profiles, before applying NBI, the density profiles have very similar shape, although the T plasma has higher density, figure 12(a). Just after the L-H transition, this changes with the peakedness becoming higher for the D plasma. The difference increases later in the discharges as the core density in the D pulse increases more rapidly than the T-pulse, figure 12(c). Before re-ionisation issue happens, the gas flow is increased again at 10.5s, the increased gas flow didn't manage to increase the core density, the particles start to accumulate at the edge and significantly escalates the density across the separatrix, as in figure 12(d). The density profile in the SOL region is completely flat and doesn't decay exponentially, figure 11(c).

For both the JET T pulses with SOL density shoulders, filamentary structures are observed in visible camera images which appear to interact with the limiter in the region associated with excessive power loads due to re-ionization, figure 13. (The shift in the imaging of figure 13 between top and bottom halves is due to in-vessel mirrors arranged to provide different vertical viewing angles for the top and bottom halves of the image.) Such filamentary structure and interaction with the first wall are only observed for these pulses with SOL density shoulder. No such structure can be observed for those without SOL density shoulders. The fact that only the pulses with flat SOL density profiles are observed to have filamentary structures implies that there are many more neutrals in the SOL region to interact with the plasma filaments and emit photons. The divertor D_α is also significantly increased when the density forms a flat shoulder. However, as there are no diagnostics to measure the features of filament/blob, it is impossible to tell whether the filamentary condition has changed before and during the re-ionisation issue.

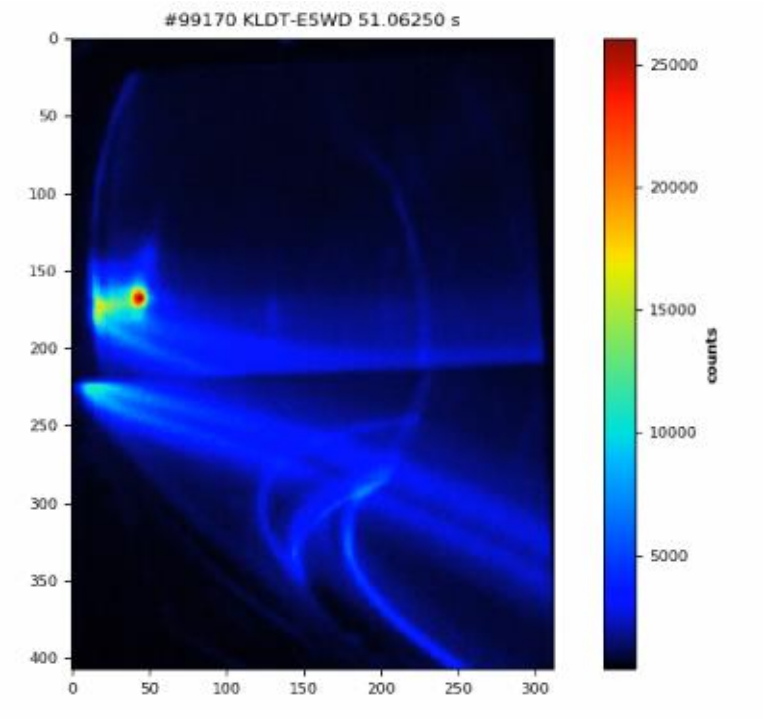

Figure 13. Filamentary structure observed for #99170 in imaging camera.

The SOL collisionality for #99170 is $\nu^*_{SOL} \approx 11$, which lies within the range of T pulses without density shoulder formation in figure 8. This suggests that the increased collisionality itself is not sufficient for the establishment of density shoulder. As mentioned in the introduction, previous studies of density shoulder formation have focused on L-mode plasma, with little evidence of density shoulders in the SOL region for H-mode plasma. SOL density shoulders in JET-ILW H-mode plasma have been first reported previously [26], but the density shoulders were rather small. The greatly extended density profiles reported here, have not been observed on JET before and are similar to those first observed on AUG with warm cryo-pump [38]. In the AUG plasma, see figure 9 in reference [38], the temperature and density profiles evolve

with continuous increasing of density with warm cryo-pump. In contrast to the usual observation for H-mode plasma with cold cryo-pump, the SOL density profile first becomes almost completely flat, and the two-zone (near SOL and far SOL) structure of the SOL density profile is broken, while that of the SOL temperature profile remains. At some point, the temperature profile becomes broader in the near SOL region, but the two-zone structure is maintained. When the cryo-pump is cold and the pumping efficiency in the divertor is high, the density and temperature decay length in the near SOL region increases $\approx 2-3$ times when collisionality reaches a critical value and there is no density shoulder formed in the SOL region. The fact that a change of pumping efficiency plays a role in the density shoulder formation, together with evidence presented here on JET T H-mode plasma, supports the hypothesis that the two types of SOL broadening have different onset condition. Increasing the edge collisionality will enhance the cross-field transport across the separatrix and thus broaden the particle and heat decay width in the near SOL region. For the formation of SOL density shoulder, the increased collisionality is not enough, change of other conditions such as neutral pressure or divertor recycling as the previous studies on TCV [25] and JET [26] is also needed.

3.3 Impact of SOL broadening on JET plasma operation

3.3.1 Unfavourable impact on NBI re-ionisation

As demonstrated in figure 9, at given gas injection level, near identical density profiles as D-reference pulse can be achieved in Ohmic plasma for JET T-plasma, it is challenging to reproduce the density profile in NBI H-mode plasma. Tritium H-mode plasma tend to have less peak core density profile and a greater opacity at the edge than their D references. This result is consistent with the previous studies on core density peaking [39] [40] [41], with an inverse correlation between core density profile peaking and global collisionality. In addition, increased gas flow is used in some T pulses to flush out

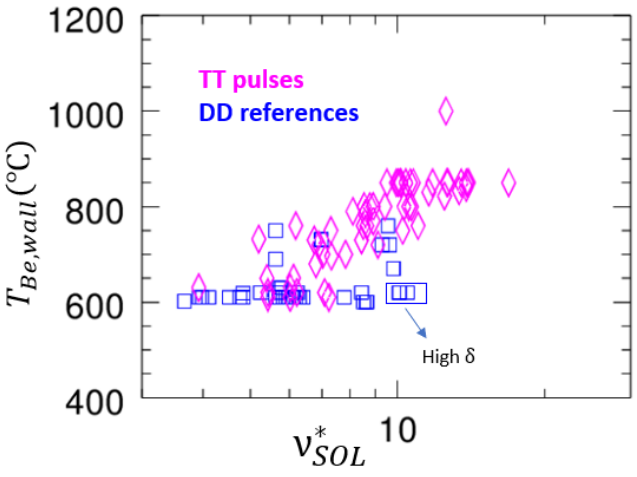

Figure 14. Wall surface temperature (BEION4) caused by re-ionisation issue against total NBI heating power. Blue squares are DD reference pulses and magenta diamonds are TT pulses. T pulses in circle are terminated by other protection at early phase.

the impurities by modifying the ELMy frequency. In T H-mode plasma, the fuelling efficiency of the increased gas appears to be lower than that in D-plasma. As can be seen in figure 7(a) and figure 11(a), the density profile shifts outwards as density increases. This is likely due to the higher edge density and resulting higher neutral opacity, which reduces the ability of neutrals to penetrate the confined region [42]. As a result, the ionisation profile is expected to move outward and increases the ionisation source in the SOL region, resulting in higher edge collisionality. The high edge collisionality enhances the cross-field transport and the SOL becomes broader when collisionality exceeds a critical level. Higher particle flux towards the edge of the plasma and the first wall would be expected to enhance the recycling flux and increase the ion and neutral densities at the edge. Those ions and neutrals provide particle seeds to re-ionize the fast beam neutrals and cause the power load issue on the wall. This picture is consistent with the observed Be wall temperature for the T pulses, as in figure 14, the power load increases with collisionality.

For D plasma, the wall temperature induced by re-ionisation appears to be lower, even at comparable collisionality. Figure 15 shows the correlation between the neutral pressure in the main chamber and separatrix density and collisionality. Here, the neutral pressure is measured in the pumping chamber, but is found to be good proxy for main chamber neutral pressure. The neutral pressure correlates positively with both separatrix density and SOL collisionality for T and D plasma. At similar collisionality, $\nu^*_{SOL} \approx 10$, the neutral pressure has a similar range for both species. The re-ionisation rate for fast beam neutrals being similar for hydrogenic species at similar collisionality.

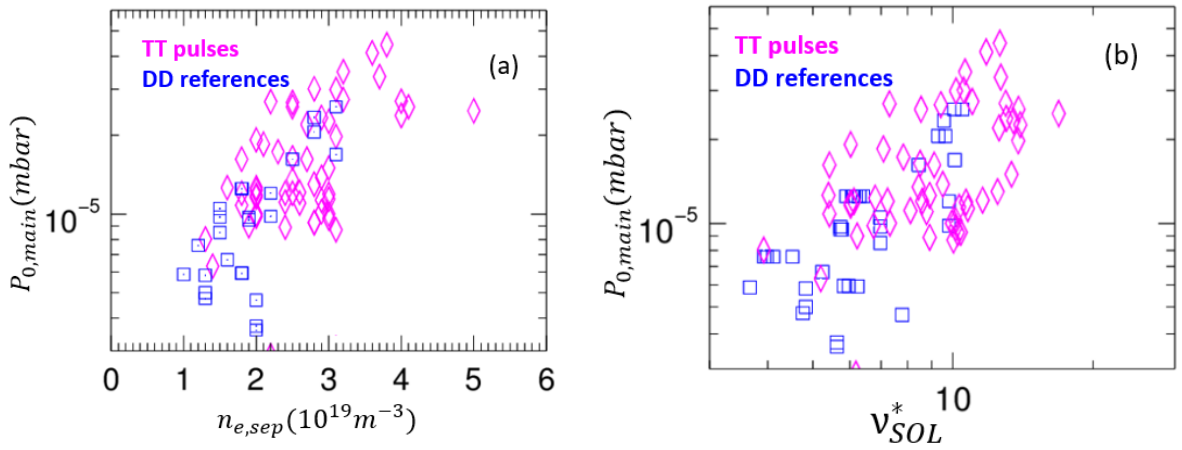

Figure 15. Main chamber neutral pressure versus (a) separatrix plasma electron density; and (b) effective SOL collisionality, ν_{SOL}. Blue squares are DD reference pulses and magenta diamonds are TT pulses.*

When the fast neutrals are ionized in the SOL region, they reflect due to the gyrate motion. If their ion Larmor radius of these fast ions is significantly smaller than the radial distance between where they are created and the Beryllium limiter, they will be largely confined. If the distance to the limiter is less than the beam ion Larmor radius, they impact the wall. Using the typical values on JET, $B_T \approx 3\,T$ and $T_{beam} \approx 100\,keV$, the typical Larmor radius for beam fast ions are, $\rho_{l,T} \approx 3.1\,cm$ for T beam and $\rho_{l,D} \approx 2.5\,cm$ for D beam. In JET, to ensure good ICRH coupling, the outer gap between separatrix and the wall is usually $5 - 5.5\,cm$. The SOL density decay length for typically $10 - 20\,mm$ for JET D reference pulses and 20-30 mm for many selected T pulses. For D plasma, the outer gap ($5 - 5.5\,cm$) is general larger than the density decay length plus D fast ion Larmor radius ($3.5 - 4.5\,cm$). For T plasma, the larger fast ion Larmor radius and SOL density decay length means that this is not the case and the expected losses of fast ions to the wall will be larger. This is also consistent with the observation that most pulses that were terminated due to re-ionisation had outer gap less than $6\,cm$. The D pulses in blue rectangle are from integrated seeded scenario experiment which have very high triangularity. These pulses have an outer gap with $5.5\,cm$, the re-ionisation doesn't cause power load issue in the D pulses. However, the T pulses built on these pulses have worst re-ionisation issue when the gap is maintained as $5.5\,cm$. This was largely mitigated by increasing the outer gap to $7.5 - 8\,cm$, an approach used widely in the later phase of the JET T campaign. However, in some cases, even with increased outer gap, the pulses still experienced excessive re-ionisation because the SOL density profile is significantly broader, such as a completely flat shape, i.e many particles manage to reach the wall instead of exhausting to the divertor. The JET T plasma with the worse excessive re-ionisation is due to the combining effect of broader SOL width and larger fast ion Larmor radius.

3.3.2 **Favourable impact on divertor target temperature**

Across the collected dataset, figure 16, it is found that, for D plasma, the core density is generally proportional to the pedestal and separatrix density, with $\frac{n_{e,core}}{n_{e,ped}} \approx 1.3\ and\ \frac{n_{e,core}}{n_{e,sep}} \approx 3$. For the T pulses, there is no clear trend and the core density seems to be saturated at $\approx 9 \times 10^{19}\,m^{-3}$ even as the pedestal and separatrix density increase significantly. The correlation between separatrix and pedestal density and its impact on JET fusion performance has been studied previously [43] [44]. High separatrix density is favourable for achieving a highly dissipative regime and is beneficial for the divertor power exhaust [45]. Across the full dataset here, with a wide range of global plasma parameters, configuration, and divertor

sweeping scenario, the maximum divertor surface temperature normalised to NBI power generally decreases with increase separatrix density, figure 17. This is consistent with two-point model prediction that the divertor plasma temperature decreases rapidly with increasing separatrix density. In addition, the broadening of SOL temperature and density profiles help spreading the power over a larger area. As JET T plasma have generally higher separatrix density than their D-references, the maximum temperature rise of the divertor surface is generally much lower, figure 3(b).

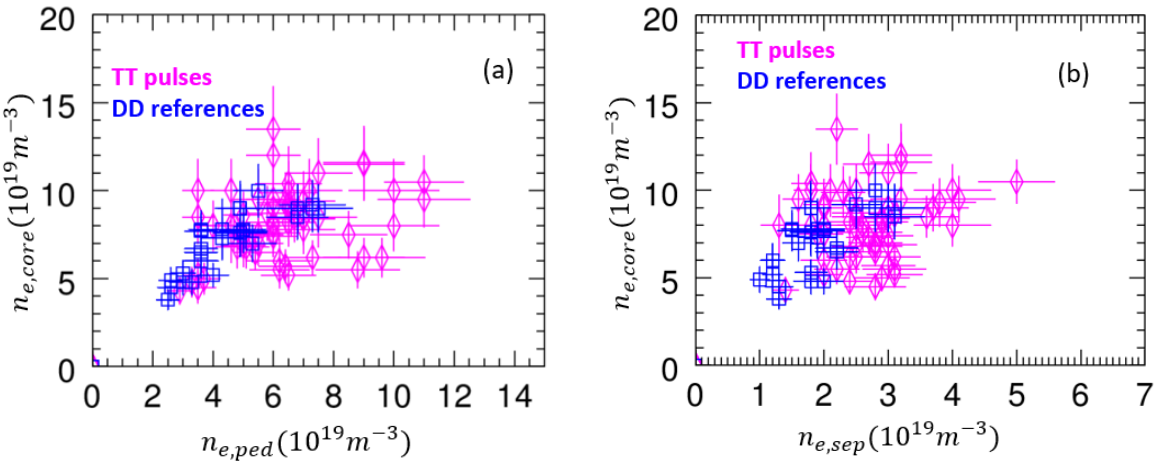

Figure 16. (a) plasma core density ($\rho \approx 0.2$) against plasma pedestal density. (b) plasma core density against plasma separatrix density. Blue squares are DD reference pulses and magenta diamonds are TT pulses.

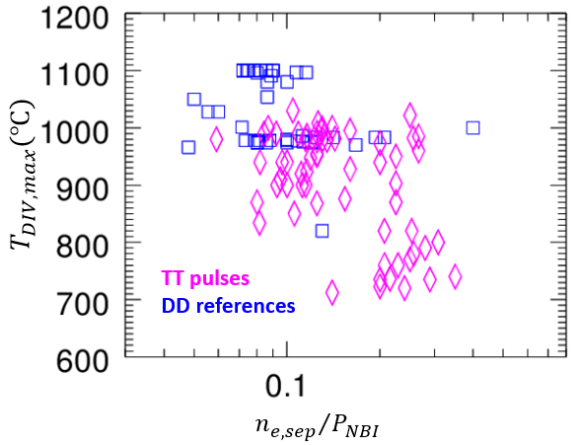

Figure 17. Maximum divertor target surface temperature against the plasma separatrix density normalized by total NBI heating power.

4 Summary and implication for future studies

The unusually high level of discharges terminated by excessive NBI re-ionisation during the recent JET T campaign motivated the study of the SOL changes of these discharges. A dataset of 72 T pulses, 18 of which terminated due to excessive power load by NBI re-ionisation issue, and their D references was compiled. Comparing the T pulses which are terminated due to re-ionisation with their D reference pulses, it is found that the separatrix density is higher and the SOL profiles are broader in the T pulses. The separatrix collisionality in T plasma is generally higher than their D references.

The majority of T pulses studied (70), and all of the D references, exhibit radially exponentially decaying SOL density and temperature profiles. At low collisionality, the SOL profiles have SOL width of $\lambda_{n_e} = 10 - 20mm$ in the near SOL region and at high collisionality, this becomes $\approx 2 - 3$ times broader, with both λ_{n_e} and λ_{T_e} broadened at a similar level. This is consistent with previous AUG observations in D plasma [2] [6].

The other two JET T pulses studied displayed a completely flat density profile with over an order of magnitude broader λ_{n_e} and can be identified as exhibiting so-called '*density shoulder formation*' [18] [20]. The SOL temperature profile for these discharges is radially exponentially decaying but has roughly 3 times broader λ_{T_e} than other similar discharges. Clear filamentary structures are observed when the density shoulder is formed, suggesting a much higher neutral density in the SOL region. The SOL collisionality of the pulses with density shoulder formation lies within the range of those without density shoulder. Increasing collisionality above a certain level will enhance the cross-field transport across the separatrix and broaden the near SOL profiles to a certain level. However, it appears insufficient to for '*density shoulder formation*' in the SOL as many T pulses at similar and higher collisionality do not exhibit density shoulder formation. Additional physics, such as neutral interaction or divertor recycling, must be required as indicated in previous studies by Vianello on TCV and Wynn on JET [25] [26].

Broader SOL profiles, due to the enhanced cross-field transport, provide more particles to ionize the Beam fast neutrals. However, re-ionisation in T plasma is associated with higher limiter power loads than D plasma even for plasma with similar SOL collisionality. The larger limiter power loads due to re-ionisation observed in the T pulses relative to their D references has been shown to be consistent with the combined effects of the broadening of the SOL profile and beam ion Larmor radius. In contrast, the escalated separatrix density and broader SOL width is beneficial for the power exhaust in the divertor by increasing the parallel temperature

gradient in the SOL and spreading the head loads to the larger area. Thus, JET T H-mode plasma have much cooler divertor target than D plasma at given NBI heating power.

Near identical density profiles can be achieved for T and D plasma with identical gas fuelling and configuration in the Ohmic phase, but, in H-mode soon after applying NBI heating, the core density peaking is reduced in T plasma and more particles accumulate at the pedestal and separatrix region. This implies that the difference at the separatrix and SOL between T and D plasma originates from the confined plasma region. Higher collisionality increase the opacity at the edge of the confined plasma region and reduces the fuelling efficiency for gas injection and recycling, which further escalates the edge collisionality and eventually changes the SOL profiles.

Excessive re-ionisation leading to heating of the Be wall is not unique to pure T plasma. The D references in this study were deliberately chosen as high performing discharges without major beam reionisation power loads. In previous D plasma, there are certainly plasma, such as those in H-mode density limit studies, which have a highest re-ionisation risk on JET. And, in the following DT campaign, re-ionisation causes power load on Beryllium limiter in some pulses too. For discharges in the JET DT campaign, there is evidence that power load issue caused by re-ionisation issue can be mitigated after a certain amount of neon is injected into high-triangularity plasma. Apart from the well-known benefit of integrating high core performance and heat load control, integrated high performance seeded scenario [46] [47] may provide solution for mitigating beam re-ionisation issue.

ITER will operate in high edge density to enable completely or partial detachment in the divertor. Operation at high SOL density and collisionality will be likely associated with broad SOL profiles and so beneficially reduced divertor heat loads. In addition to the usual concern from enhanced cross-field transport for fusion reactors - increased sputtering of the first wall components and tritium (T) inventory - any future burning plasma devices with NBI heating, will also experience an increased risk of excessive reionisation drive heat loads at the limiters. These effects will be particularly acute for SOL exhibiting density shoulders.

The work presented here will be extended to a wide range of Deuterium plasma and DT plasma to study enhanced cross-field transport with various cryo-pump condition and impurity seeding conditions and in the presence of DT. The high heat loads observed for SOL with density shoulders make the understanding and prediction of this phenomena particularly desirable to ensure good ITER operation.

Acknowledgements

This work has been carried out within the framework of the EUROfusion Consortium, funded by the European Union via the Euratom Research and Training Programme (Grant Agreement No 101052200 — EUROfusion) and from the RCUK [grant number EP/T012250/1. Views and opinions expressed are however those of the author(s) only and do not necessarily reflect those of the European Union or the European Commission. Neither the European Union nor the European Commission can be held responsible for them.

References

[1] T. Eich et al, *Phys. Rev. Lett.*, vol. 107, p. 215001, 2011.

[2] H. J. Sun et al, *Plasma Phys. Contr. Fusion*, vol. 57, p. 075005, 2015.

[3] H. J. Sun et al, *Plasma Phys. Control. Fusion*, vol. 61, p. 014005, 2019.

[4] M. Faitsch et al, *Plasma Phys. Control. Fusion*, vol. 62, p. 085004, 2020.

[5] D. Silvagni et al, *Plasma, Phys. Control. Fusion*, vol. 62, p. 045015, 2020.

[6] T. Eich, P. Manz and R. Goldston et al, *Nucl. Fusion*, vol. 60, p. 056016, 2020.

[7] N. M. Li, X. Q. Xu and R. J. Goldston et al, *Ncul.Fusion*, vol. 61, p. 026005, 2021.

[8] A. Brown and R. Goldston, *Nuclear Materials and Energy*, vol. 27, p. 101002, 2021.

[9] C. Chang et al, *Nucl. Fusion*, vol. 57, p. 116023, 2017.

[10] Y. Xu et al, *Nucl. Fusion*, vol. 51, p. 063020, 2011.

[11] R. Singh et al, *Nucl. Fusion*, vol. 61, p. 076009, 2021.

[12] R. Hajjar et al, *Phys. Plasma*, vol. 25, p. 062306, 2018.

[13] T. Long et al, *Nucl. Fusion*, vol. 61, p. 126066, 2021.

[14] B. N. Roger, J. F. Drake and A. Zeiler, *Physical Review Letters*, vol. 81, pp. 4396-4399, 1998.

[15] M. Tokar et al, *Phys. Rev. Lett*, vol. 91, p. 095001, 2003.

[16] X. Q. Xu, W. M. Nevins and T. D. Rognlien, *Physics of Plasmas*, vol. 10, pp. 1773-1781, 2003.

[17] K. Mccordmick et al, *J. Nucl. Mater.*, vol. 196, p. 264, 1992.

[18] B. Lambombard et al, *Phys.Plasmas*, vol. 8, p. 2107, 2001.

[19] O. Garcia et al, *Plasma Phys. Control. Fusion,* vol. 48, p. L1, 2006.

[20] D. Carralero et al, *Phys. Rev. Lett,* vol. 115, p. 215002, 2015.

[21] J. Boedo et al, *Phys. Plasmas,* vol. 8, p. 4826, 2001.

[22] D. Carralero et al, *Nucl. Fusion,* vol. 57, p. 056044, 2017.

[23] F. Militello et al, *Plasma Phys. Control. Fusion,* vol. 55, p. 025005, 2013.

[24] F. Militello et al, *Nucl.Fusion,* vol. 56, p. 104004, 2016.

[25] N. Vianello et al, *Nucl. Fusion,* vol. 57, p. 116014, 2017.

[26] A. Wynn et al, *Nucl. Fusion,* vol. 58, p. 056001, 2018.

[27] B. Lipschultz et al, *Nucl. Fusion,* vol. 47, p. 1189, 2007.

[28] D. Carralero et al, *Nucl. Fusion,* vol. 58, p. 096015, 2018.

[29] M. Griener et al, *Nuclear Materials and Energy,* vol. 25, p. 100854, 2020.

[30] U. Stroth et al, *Nucl.Fusion,* vol. 62, p. 042006, 2022.

[31] G. Arnoux et al, *Rev. Sci. Instrum,* vol. 83, p. 10D727, 2012.

[32] A. Huber et al, *Nucl. Fusion,* vol. 58, p. 106021, 2018.

[33] E. Joffrin and e. al, *Nucl. Fusion,* vol. 59, p. 112021, 2019.

[34] J. Maillous and e. al, *Nucl. Fusion,* vol. 62, p. 042026, 2022.

[35] R. Pasqualotto, *Review of Scientific Instruments* , vol. 75, p. 3891, 2004.

[36] L. Frassinetti, M. Beurskens and R. Scannell et al, *Review of Scientific Instruments,* vol. 83, p. 013506, 2012.

[37] H. J. Sun et al, *Nucl. Fusion,* vol. 61, p. 066009, 2021.

[38] H. J. Sun et al, *Plasma Phys. Control Fusion,* vol. 62, p. 025005, 2020.

[39] H. Weisen et al, *Nucl. Fusion,* vol. 45, pp. L1-4, 2005.

[40] M. Maslov et al, *Nucl. Fusion,* vol. 49, p. 075037, 2009.

[41] T. Tala et al, *Nucl. Fusion,* vol. 59, p. 126030, 2019.

[42] S. Mordijck et al, *Nucl. Fusion,* vol. 60, p. 082006, 2020.

[43] L. Frassinetti et al, *Nucl. Fusion,* vol. 61, p. 126054, 2021.

[44] A. Leonard et al, *Nucl. Fusion,* vol. 57, p. 086033, 2017.

[45] P. Stangeby, The Plasma Boundary of Magnetic fusion devices, London: IOP Publishing, 2000.

[46] C. Giroud et al, *Plasma Phys. Control Fusion,* vol. 57, p. 035004, 2015.

[47] C. Giroud et al, in *IAEA FEC*, Nice, France, 2021.